A cyclic RGD-coated peptide nanoribbon as a selective intracellular nanocarrier†

Yong-beom Lim,[a] Oh-Joon Kwon,[b] Eunji Lee,[a] Pyung-Hwan Kim,[b] Chae-Ok Yun[b] and Myongsoo Lee*[a]

Received 13th February 2008, Accepted 7th March 2008
First published as an Advance Article on the web 9th April 2008
DOI: 10.1039/b802470g

We have synthesized a peptide-based supramolecular building block consisting of a cyclic Arg-Gly-Asp (cRGD) peptide segment and a β-sheet-forming peptide segment. The block peptide was shown to self-assemble into a cRGD-coated nanoribbon structure, as revealed by circular dichroism (CD), dynamic light scattering (DLS), and transmission electron microscopy (TEM) studies. We have shown that this cRGD-coated nanoribbon can encapsulate hydrophobic guest molecules and deliver them into cells. Colocalization of the nanoribbon with LysoTracker and the selective intracellular delivery results suggests that the cRGD-coated nanoribbon is likely to be internalized into the cells through integrin receptors.

Introduction

Self-assembled nanostructures have great potential to be utilized in many types of biotechnological applications.[1–4] Generation of precisely defined and controllable nanostructures has been possible by rational design of supramolecular building blocks.[5–7] Among the various types of building blocks, those based on peptides have increasingly been investigated. One of the fundamental advantages of peptide-based building blocks is that their constituent amino acids are bio-derived biocompatible materials. Moreover, the immense amount of information on protein structure and folding currently available can be adapted in designing the shape and size of peptide supramolecular nanostructures. Examples of peptide-based nanostructures include a variety of micelles from peptide amphiphiles,[8,9] coiled-coils from α-helical peptide bundles,[10] nanotubes from cyclic peptides,[11] nanotubes and nanocages from dipeptides,[12] vesicular structures from diblock peptides of polyarginine and polyleucines,[13] thermoresponsive elastin-like aggregates,[14] closed-micelles from peptide-PEG block copolymers,[15] and nanofibers from β-sheet peptides.[16–24]

Among them, β-sheet peptides are suitable for constructing 1-dimensional (1D) nanoribbon structures (β-ribbons).[16–24] Compared to spherical nanostructures, 1D nanostructures have certain advantages in that they persist longer *in vivo*[25] and can be used in agglutinating cells.[23,24] Rational design of β-sheet peptide building blocks has made it possible to prevent lateral aggregation, to control the length of 1D β-ribbons, and to switch between aggregated and disaggregated states. One of the important issues in developing supramolecular biomaterials is their functionalization. It has been shown that β-ribbons can encapsulate hydrophobic guest molecules in the interfacial space within the ribbon and, when functionalized with the cell-penetrating peptide (CPP) Tat, efficiently deliver guests into cells.[22] Although the advantage of CPPs is their efficient cell internalization, they lack cell specificity. Therefore, it is a question whether β-ribbons can be functionalized to become specific to certain cell types, such as cancer cells.

As an example of specific delivery, we explore here the RGD–integrin system. The $\alpha_v\beta_3$ integrin receptor is expressed only on proliferating endothelial cells such as those present in growing tumors.[26] The $\alpha_v\beta_3$ integrin is one of the most specific markers of tumor vasculature and is an attractive candidate in cancer-targeting strategies.[27] It has been shown that small peptides containing the Arg-Gly-Asp (RGD) amino acid sequence specifically bind to $\alpha_v\beta_3$ integrin.[28] Thus, there has been growing interest in targeting RGD conjugates for drug delivery, gene delivery, and imaging applications. The multivalent presentation of RGD on nanoparticles has been shown to enhance its binding affinity to endothelial cells and extend its blood half-life.[29] In this regard, the self-assembly of RGD peptides would be an effective way of achieving multivalent presentation of RGD peptides. Inspired by these facts, here we investigate whether 1D β-ribbons can be functionalized to become a cancer-cell-specific and multivalent drug carrier by coating it with RGD peptides.

Results and discussion

Synthesis of supramolecular building blocks

The linear precursor peptide was synthesized on Rink amide MBHA resin using standard Fmoc protocols (Scheme 1a). Small peptides such as RGD generally possess a very high conformational flexibility. For this reason, cyclization of RGD has been shown to be effective in limiting the conformational flexibility, consequently lowering the unfavorable entropy loss upon binding.[30,31] Cyclization of RGD was performed by intramolecular *S*-alkylation, in which the thiol group of the cysteine residue displaces bromide from the *N*-terminal bromoacetyl group to form a cyclic thioether peptide.[32] The cyclization reaction was performed while the protected peptide was bound to the resin to achieve a 'pseudo-dilution' effect.[33] This synthetic approach required an appropriate orthogonal protection strategy for the side chain thiol

[a]*Centre for Supramolecular Nano-Assembly, Department of Chemistry, Yonsei University, Shinchon 134, Seoul, 120-749, Korea. E-mail: mslee@yonsei.ac.kr; Fax: +82 2 393 6096; Tel: +82 2 2123 2647*
[b]*Brain Korea 21 Project for Medical Science, Institute for Cancer Research, Yonsei Cancer Centre, Yonsei University College of Medicine, Seoul, Korea*
† Electronic supplementary information (ESI) available: CD and DLS spectra; CLSM image. See DOI: 10.1039/b802470g

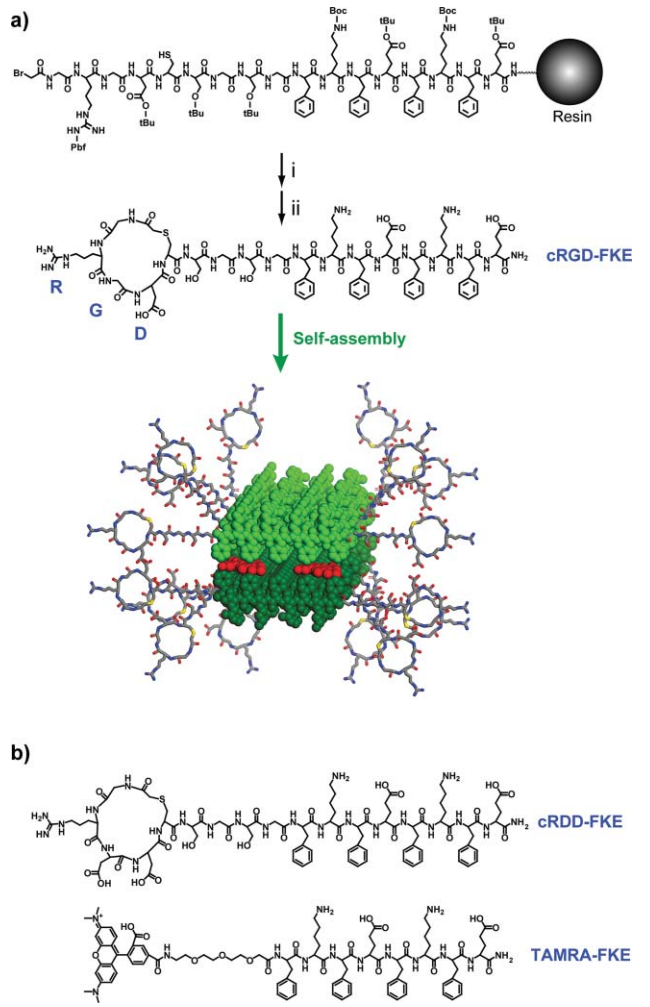

Scheme 1 (a) Synthesis of cRGD-FKE and a model of β-ribbon formation by self-assembly. The model was constructed by using Materials Studio 4.0. (i) 1% DIPEA in NMP; (ii) 95% TFA, 2.5% 1,2-ethanedithiol, 2.5% thioanisole. Hydrophobic guest molecules (red) are shown to be encapsulated within the cRGD-FKE β-ribbon. Pbf: 2,2,4,6,7-pentamethyldihydrobenzofuran-5-sulfonyl, tBu; *t*-Butyl, Boc; *t*-butyloxycarbonyl. (b) Structures of cRDD-FKE and TAMRA-FKE. TAMRA; 5-carboxytetramethylrhodamine.

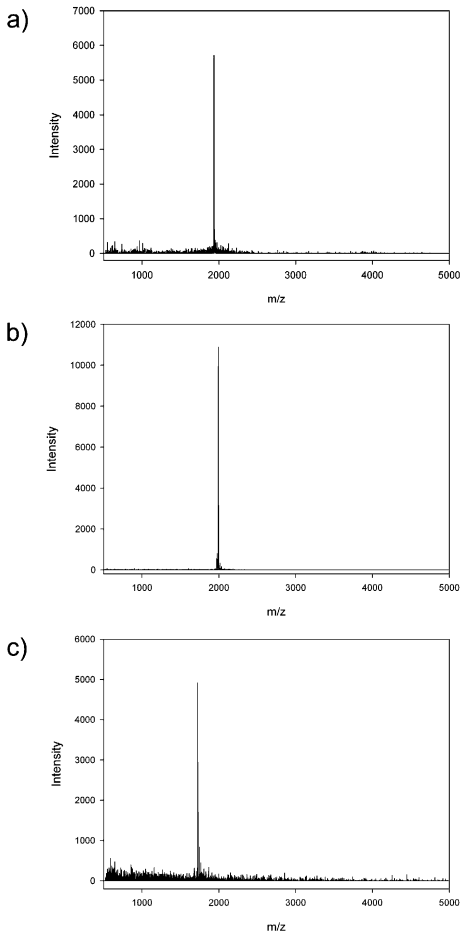

Fig. 1 MALDI-TOF MS spectra of (a) cRGD-FKE, (b) cRDD-FKE, and (c) TAMRA-FKE.

of the cysteine, which would allow selective deprotection of this residue without removing side chain-protecting groups of the other residues or cleaving the linear precursors from the resin. To this end, the methoxytrityl (Mmt)-protected cysteine was employed during the linear precursor synthesis, which can be selectively removed by the treatment with 1–2% TFA without affecting the side chain protecting groups in other amino acids.[34] The cyclization reaction commenced by the exposure of the resin-bound peptide to 1% DIPEA/NMP. The resin-bound cyclized product was liberated from the resin by treatment with cleavage cocktail (95% TFA, 2.5% 1,2-ethanedithiol, 2.5% thioanisole) and purification by reverse-phase HPLC, yielding cRGD-FKE. The molecular weight was confirmed by MALDI-TOF mass spectrometry (Fig. 1). The purity of the peptides was >95% as determined by analytical HPLC. cRGD-FKE consists of a cRGD segment, a flexible linker segment (Ser-Gly-Ser-Gly; SGSG), and a β-sheet-forming segment (Phe-Lys-Phe-Glu-Phe-Lys-Phe-Glu; FKFEFKFE). A control building block, cRDD-FKE, was synthesized similarly (Scheme 1b). It has been shown that $(FKFE)_n$ peptides form a β-ribbon structure upon self-assembly.[16,22–24]

Self-assembly of the peptide building blocks

The formation of β-ribbons was studied by circular dichroism (CD), transmission electron microscopy (TEM), and dynamic light scattering (DLS). CD spectrum showed negative minimum of ellipticity at 214 nm, which indicates the presence of β-sheet interaction (Fig. 2a). Another negative minimum around 200 nm is likely to come from a flexible structure, such as the linker segment. The β-sheet interaction drove the formation of a discrete β-ribbon structure, as revealed by TEM investigation (Fig. 2b). DLS investigation showed that the size of the β-ribbon is distributed from several hundred nanometres to more than a micrometre (Fig. 2c). Although analysis of β-sheet fibers by DLS is often not straightforward,[35] we can get a rough estimate of size distribution of the fibers by DLS.

Intracellular delivery

We next investigated whether cRGD-FKE β-ribbons can efficiently be internalized into the cell. To visualize the internalization, we synthesized a fluorescently labeled β-sheet peptide (TAMRA-FKE) in which the cRGD segment of cRGD-FKE was replaced by

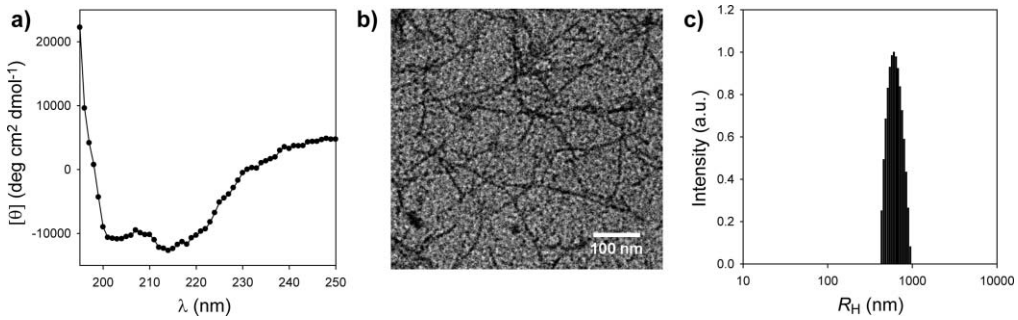

Fig. 2 Self-assembly of cRGD-FKFE to form cRGD-coated β-ribbons. a) CD spectrum of cRGD-FKE. b) TEM micrograph of the β-ribbons. c) Distribution of hydrodynamic radius (R_H) of the β-ribbons by DLS. The average R_H was 605 nm.

5-carboxytetramethylrhodamine (Scheme 1b). cRGD-FKE and TAMRA-FKE were co-assembled[22,36] at a 200 : 1 ratio, and the co-assembled β-ribbon was incubated with mammalian cells (HeLa). CD and DLS analyses show that the β-sheet nanostructures are well preserved after the co-assembly process (Fig. S1†). Confocal laser scanning microscopy (CLSM) image of the treated cells showed that the β-ribbons efficiently entered into the cells (Fig. 3a). The β-ribbons existed mostly in the cytoplasmic compartment. The punctual distribution pattern suggests an endocytic entry pathway.[37] To corroborate the endocytic entry mechanism, a co-localization study was performed with LysoTracker (Fig. 3b,c). LysoTracker is an acidotropic reagent for labeling and tracing acidic organelles such as late endosomes and lysosomes in live cells. As shown in Fig. 3c, a substantial fraction of the red fluorescence from the β-ribbons co-localizes (yellow) with the fluorescence from LysoTracker (green), further confirming endocytic entry of the β-ribbon. The endocytic entry mechanism suggests that the cRGD-coated β-ribbon is likely to be internalized through integrin receptors.

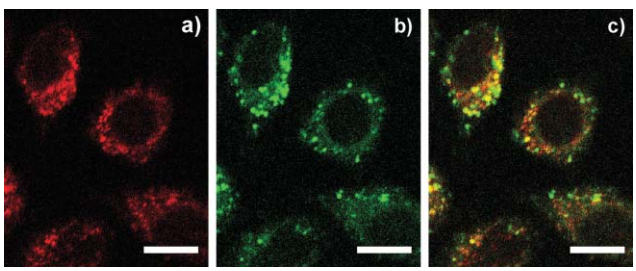

Fig. 3 Endocytic cell entry of cRGD-FKFE. (a) Red fluorescence from co-assembled cRGD-FKE/TAMRA-FKE β-ribbon. (b) Green fluorescence from LysoTracker Green DND-26. (c) Overlay of (a) and (b). Scale bar: 50 μm.

To address the potential of cRGD-coated β-ribbons as a drug carrier specific for the integrin receptor, hydrophobic guest molecules (Nile red) were encapsulated within the β-ribbon, and intracellular delivery potency was investigated. As shown in Fig. 4, red fluorescence from Nile red was distributed over the entire cytoplasmic compartment of the cells when the cells were treated with Nile red-encapsulated cRGD β-ribbons. The result indicates efficient intracellular drug delivery potency of the β-ribbon. Next, we asked whether the RGD peptide sequence showed specificity. For this purpose, cRDD-FKE peptide was synthesized as a negative control (Scheme 1b). The cRGD-FKE β-ribbon or

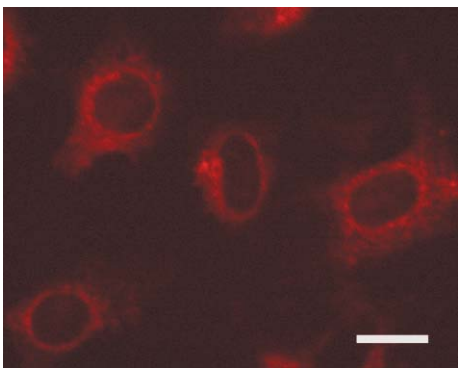

Fig. 4 Intracellular delivery of encapsulated Nile red in HeLa cell. Scale bar: 50 μm.

cRDD-FKE β-ribbon was encapsulated with the same amount of Nile red, and added to Jurkat cells. The Jurkat cell line has been reported to have a large number of integrin receptors and was able to bind to RGD-containing peptide.[38] Fluorescence-activated cell sorter (FACS) analysis of Nile red delivery shows that cRGD-FKE β-ribbon has much higher delivery activity than cRDD-FKE β-ribbon (Fig. 5). Quantitative analysis of fluorescence from the cells in the boxed region, R1, shows that the Nile red delivery efficiency of cRGD-FKE β-ribbon is about 5 times higher than that of cRDD-FKE β-ribbon. The RGD sequence-specific delivery of the hydrophobic guests suggests that RGD-coated β-ribbon can be developed as a drug delivery carrier specific for the integrin receptor.

In conclusion, we have shown that peptide β-ribbons can be functionalized to become a selective intracellular drug delivery carrier. Given the biocompatible nature of peptide β-ribbons' constituent amino acids and their unique 1D shape, they have potential to be developed as biocompatible, specific, and versatile nanocarriers. Moreover, this finding should lead to the wide utilization of β-sheet peptide nanoribbons in various biological applications that require both functionality and specificity.

Experimental

Syntheses of cyclic peptides

Linear precursor peptide was synthesized on Rink amide MBHA resin using standard Fmoc protocols on an Applied Biosystems model 433A peptide synthesizer. The sequences of the linear

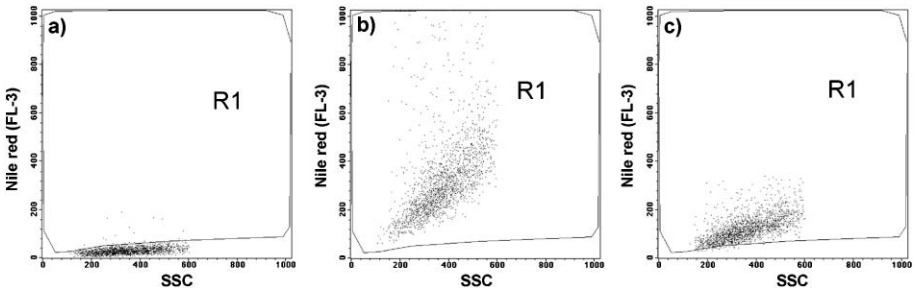

Fig. 5 Selective delivery of hydrophobic guest molecules. FACS analysis of (a) Jurkat cells, (b) Jurkat cells treated with Nile red-encapsulated cRGD-FKE β-ribbons, and (c) Jurkat cells treated with Nile red-encapsulated cRDD-FKE β-ribbons. One mol% of Nile red was encapsulated relative to that of the peptides. The cells were treated with the Nile red-encapsulated β-ribbons (10 μM) for 3 h.

precursors for cRGD-FKE and cRDD-FKE syntheses were GRGDCSGSGFKFEFKFE and GRDDCSGSGFKFEFKFE, respectively. Standard amino acid protecting groups were employed except cysteine, in which an acid-labile methoxytrityl (Mmt) group was used. The peptide-attached resin (20 μmol of N-terminal amine groups) was swollen in *N*-methyl-2-pyrrolidone (NMP) for 30 min. Before addition to the resin, a mixture of bromoacetic acid (28 mg, 200 μmol) and *N*,*N*′-diisopropylcarbodiimide (15.5 μL, 100 μmol) in NMP was incubated for 10 min for carboxyl activation. The reaction was continued for 1 h with shaking at room temperature. The reaction was performed in a 6 mL polypropylene tube with a frit (Restek, USA). The resin was then washed successively with NMP and dichloromethane (DCM). For orthogonal deprotection of the Mmt group from the cysteine, the resin was treated with 1% trifluoroacetic acid (TFA)–5% triisopropylsilane (TIS)–DCM (2 mL) several times (~10 × 1 min) until the yellow color in the solution disappeared. The resin was washed and the intramolecular cyclization reaction was performed in 3 mL of 1% diisopropylethylamine (DIPEA)–NMP overnight with shaking at room temperature. The resin was then successively washed with NMP and acetonitrile, and dried *in vacuo*. The dried resin was treated with cleavage cocktail (TFA–1,2-ethanedithiol–thioanisole; 95 : 2.5 : 2.5) for 3 h, and was triturated with *tert*-butyl methyl ether. The peptides were purified by reverse-phase HPLC (water–acetonitrile with 0.1% TFA). The molecular weight was confirmed by MALDI-TOF mass spectrometry. The purity of the peptides was >95% as determined by analytical HPLC. Concentration was determined spectrophotometrically in water–acetonitrile (1 : 1) using a molar extinction coefficient of phenylalanine (195 M^{-1} cm^{-1}) at 257.5 nm.

Synthesis of TAMRA-FKE

Fmoc-NH-triethylene glycol-COOH[39] (13 mg, 30 μmol) was activated with HBTU (10.2 mg, 27 μmol) in NMP (2 mL) in the presence of DIPEA (10.5 μL, 60 μmol) for 10 min and then the mixture was added to a resin-bound peptide (FKFEFKFE-Rink amide MBHA resin, 10 μmol). The reaction was continued for 2 h with shaking at room temperature and the resin was washed with DMF. Fmoc was removed with 20% piperidine in DMF (30 min), followed by DMF washes. For labeling the peptide with tetramethylrhodamine (TAMRA), the resin-bound peptide was reacted with 5-carboxytetramethylrhodamine, succinimidyl ester (10.6 mg, 20 μmol) in the presence of DIPEA (7 μL, 40 μmol) in DMF (2 mL). The resin was then successively washed with NMP and acetonitrile, and dried *in vacuo*. The dried resin was treated with cleavage cocktail (TFA–1,2-ethanedithiol–thioanisole; 95 : 2.5 : 2.5) for 3 h, and was triturated with *tert*-butyl methyl ether. The peptide was purified by reverse-phase HPLC (water–acetonitrile with 0.1% TFA). The molecular weight was confirmed by MALDI-TOF mass spectrometry. The purity of the peptide was >95% as determined by analytical HPLC. Concentration was determined spectrophotometrically in water–acetonitrile (1 : 1) using a molar extinction coefficient of TAMRA (80 400 M^{-1} cm^{-1}) at 547 nm.

Circular dichroism (CD) spectroscopy

CD spectra were measured using a JASCO model J-810 spectropolarimeter. The peptide (30 μM) was dissolved in phosphate-buffered saline (PBS) and the spectrum was recorded from 250 nm to 190 nm using a 0.1 cm path-length cuvette. Scans were repeated three times and averaged. Molar ellipticity was calculated per amino acid residue.

Dynamic light scattering (DLS)

Dynamic light scattering was performed at room temperature with a ALV/CGS-3 Compact Goniometer System equipped with a He–Ne laser operating at 632.8 nm. The scattering angle was 90°. Before measurement, the sample (30 μM in PBS) was centrifuged at 16 110 *g* for 20 min to sediment any dust particles. The size distribution was determined by using a constrained regularization method.[40]

Transmission electron microscopy (TEM)

For TEM, 3 μL of an aqueous solution of sample was placed onto a holey carbon-coated copper grid, and 3 μL of 2% (w/w) ruthenium tetroxide solution was added for positive staining. The sample was deposited for 1 min, and excess solution was wicked off by filter paper. The dried specimen was observed with a JEOL-JEM 2010 instrument operating at 120 kV. The data were analyzed with DigitalMicrograph software.

Encapsulation experiment

To the dye Nile red (30 ng, 0.1 nmol) dissolved in acetonitrile (50 μL) in a microcentrifuge tube was added 50 μL of peptide (10 nmol) in water, and the solution was sonicated. The acetonitrile was evaporated by opening the microcentrifuge tube cap overnight

until the volume of the solution became about 40–50 μL. The solution was then lyophilized to dryness to remove any traces of acetonitrile. The dried residue was redissolved in water at the desired concentration.

Colocalization study

HeLa cells were seeded on sterile 12 mm diameter coverslip in 35 mm dishes (5×10^4 cells per glass), and incubated for 24 h at 37 °C. The cells on the coverslip were washed 3 times with PBS and incubated at 37 °C with the co-assembled cRGD-FKE/TAMRA-FKE β-ribbon (cRGD-FKE : TAMRA-FKE = 200 : 1). The final concentration of cRGD-FKE was 2.5 μM. Afterward, cells were washed with PBS, and treated with 500 nM LysoTracker Green DND-26 (Molecular probes, Eugene, OR) for 1 min at room temperature. After PBS washing, the coverslip was inverted and placed onto glass slides over the fluorescent mounting medium (Dako, Carpinteria, CA). The cells were visualized under a confocal microscope (LSM 510 META, Carl Zeiss, Germany).

FACS analysis of intracellular delivery of hydrophobic guest molecules

Jurkat cells (4×10^4) were seeded on 96-well plate in RPMI medium 1640. The cells were treated with Nile red-encapsulated β-ribbons (10 μM) for 3 h. The cells were then washed three times with PBS and 0.5 mL of FACS buffer (94.5% PBS, 5% cell dissociation buffer, and 0.5% FBS) was added. The Nile red fluorescence from the cells was analyzed by a FACSCalibur flow cytometer (Becton Dickinson) in FL3 channel. Typically 5×10^3 cells were sorted, and data were analyzed with CELLQUEST software. For quantification of uptake efficiency, the percentage of cells gated in the boxed region of R1 (Fig. 5) was multiplied by the Y mean value (FL3 value).

Acknowledgements

We gratefully acknowledge the National Creative Research Initiative Program of the Korean Ministry of Science and Technology for financial support of this work.

References

1 S. Zhang, *Nat. Biotechnol.*, 2003, **21**, 1171–1178.
2 H. G. Börner and H. Schlaad, *Soft Matter*, 2007, **3**, 394–408.
3 I. W. Hamley and V. Castelletto, *Angew. Chem., Int. Ed.*, 2007, **46**, 4442–4455.
4 Y.-b. Lim and M. Lee, *Org. Biomol. Chem.*, 2007, **5**, 401–405.
5 T. Shimizu, M. Masuda and H. Minamikawa, *Chem. Rev.*, 2005, **105**, 1401–1443.
6 J. A. A. W. Elemans, A. E. Rowan and R. J. M. Nolte, *J. Mater. Chem.*, 2003, **13**, 2661–2670.
7 M. Lee, B.-K. Cho and W.-C. Zin, *Chem. Rev.*, 2001, **101**, 3869–3892.
8 G. A. Silva, C. Czeisler, K. L. Niece, E. Beniash, D. A. Harrington, J. A. Kessler and S. I. Stupp, *Science*, 2004, **303**, 1352–1355.
9 Y.-b. Lim, E. Lee and M. Lee, *Angew. Chem., Int. Ed.*, 2007, **46**, 9011–9014.
10 M. M. Stevens, N. T. Flynn, C. Wang, D. A. Tirrell and R. Langer, *Adv. Mater.*, 2004, **16**, 915–918.
11 M. R. Ghadiri, J. R. Granja, R. A. Milligan, D. E. Mcree and N. Hazanovich, *Nature*, 1993, **366**, 324–327.
12 S. Ghosh, M. Reches, E. Gazit and S. Verma, *Angew. Chem., Int. Ed.*, 2007, **46**, 2002–2004.
13 E. P. Holowka, V. Z. Sun, D. T. Kamei and T. J. Deming, *Nat. Mater.*, 2007, **6**, 52–57.
14 D. W. Urry, C.-H. Luan, T. M. Parker, D. C. Gowda, K. U. Prasad, M. C. Reid and A. Safavy, *J. Am. Chem. Soc.*, 1991, **113**, 4346–4348.
15 A. Harada and K. Kataoka, *Science*, 1999, **283**, 65–67.
16 D. M. Marini, W. Hwang, D. A. Lauffenburger, S. Zhang and R. D. Kamm, *Nano Lett.*, 2002, **2**, 295–299.
17 C. W. G. Fishwick, A. J. Beevers, L. M. Carrick, C. D. Whitehouse, A. Aggeli and N. Boden, *Nano Lett.*, 2003, **3**, 1475–1479.
18 H. Dong, S. E. Paramonov, L. Aulisa, E. L. Bakota and J. D. Hartgerink, *J. Am. Chem. Soc.*, 2007, **129**, 12468–12472.
19 J. H. Collier and P. B. Messersmith, *Adv. Mater.*, 2004, **16**, 907–910.
20 J. Hentschel, E. Krause and H. G. Börner, *J. Am. Chem. Soc.*, 2006, **128**, 7722–7723.
21 J. M. Smeenk, M. B. J. Otten, J. Thies, D. A. Tirrell, H. G. Stunnenberg and J. C. M. van Hest, *Angew. Chem., Int. Ed.*, 2005, **44**, 1968–1971.
22 Y.-b. Lim, E. Lee and M. Lee, *Angew. Chem., Int. Ed.*, 2007, **46**, 3475–3478.
23 Y.-b. Lim, S. Park, E. Lee, H. Jeong, J.-H. Ryu, M. S. Lee and M. Lee, *Biomacromolecules*, 2007, **8**, 1404–1408.
24 Y.-b. Lim, S. Park, E. Lee, J.-H. Ryu, Y.-R. Yoon, T.-H. Kim and M. Lee, *Chem.–Asian J.*, 2007, **2**, 1363–1369.
25 Y. Geng, P. Dalhaimer, S. Cai, R. Tsai, M. Tewari, T. Minko and D. E. Discher, *Nat. Nanotechnol.*, 2007, **2**, 249–255.
26 M. L. Janssen, W. J. Oyen, I. Dijkgraaf, L. F. Massuger, C. Frielink, D. S. Edwards, M. Rajopadhye, H. Boonstra, F. H. Corstens and O. C. Boerman, *Cancer Res.*, 2002, **62**, 6146–6151.
27 R. Shukla, T. P. Thomas, J. Peters, A. Kotlyar, A. Myc and J. R. Baker Jr., *Chem. Commun.*, 2005, 5739–5741.
28 R. Pasqualini, E. Koivunen and E. Ruoslahti, *Nat. Biotechnol.*, 1997, **15**, 542–546.
29 X. Montet, M. Funovics, K. Montet-Abou, R. Weissleder and L. Josephson, *J. Med. Chem.*, 2006, **49**, 6087–6093.
30 D. Boturyn, J.-L. Coll, E. Garanger, M.-C. Favrot and P. Dumy, *J. Am. Chem. Soc.*, 2004, **126**, 5730–5739.
31 R. Haubner, W. Schmitt, G. Hölzemann, S. L. Goodman, A. Jonczyk and H. Kessler, *J. Am. Chem. Soc.*, 1996, **118**, 7881–7891.
32 K. D. Roberts, J. N. Lambert, N. J. Ede and A. M. Bray, *J. Pept. Sci.*, 2006, **12**, 525–532.
33 D. Maclean, J. J. Baldwin, V. T. Ivanov, Y. Kato, A. Shaw, P. Schneider and E. M. Gordon, *Pure Appl. Chem.*, 1999, **71**, 2349–2365.
34 K. Barlos, D. Gatos, O. Hatzi, N. Koch and S. Koutsogianni, *Int. J. Pept. Protein Res.*, 1996, **47**, 148–153.
35 A. Lomakin and D. B. Teplow, *Protein Pept. Lett.*, 2006, **13**, 247.
36 H. Kodama, S. Matsumura, T. Yamashita and H. Mihara, *Chem. Commun.*, 2004, 2876–2877.
37 S. Veldhoen, S. D. Laufer, A. Trampe and T. Restle, *Nucleic Acids Res.*, 2006, **34**, 6561–6573.
38 N. Assa-Munt, X. Jia, P. Laakkonen and E. Ruoslahti, *Biochemistry*, 2001, **40**, 2373–2378.
39 Y.-b. Lim, S. Park, E. Lee, H. Jeong, J.-H. Ryu, M. S. Lee and M. Lee, *Biomacromolecules*, 2007, **8**, 1404–1408.
40 T. G. Braginskaya, P. D. Dobitchin, M. A. Ivanova, V. V. Klyubin, A. V. Lomakin, V. A. Noskin, G. E. Shmelev and S. P. Tolpina, *Phys. Scr.*, 1983, **28**, 73.

